Modeling the Fate and Transport of Arsenic in Wetland Sediments

Wang, Sookyun* and Seok Soon Park

(*Department of Environmental Science and Engineering, College of Engineering,*
Ewha Womans University, Seoul, Korea)

The fate and transport of many trace metals, metalloids, and radionuclides in porous media is closely linked to the biogeochemical reactions that occur as a result of organic carbon being sequentially degraded by different microorganisms using a series of terminal electron acceptors. The spatial distribution of these biogeochemical reactions is affected by processes that are often unique and/or characteristic to a specific environment. Generic model formulations have been developed and applied to simulate the fate and transport of arsenic in two hydrologic settings, permanently flooded freshwater sediments, namely non-vegetated wetland sediments and vegetated wetland sediments. The key physical processes that have been considered are sedimentation, effects of roots on biogeochemistry, advective transport, and differences in mixing processes. Steady-state formulations were applied to the sedimentary environments. Results of numerical simulations show that these physical processes significantly affect the chemical profiles of different electron acceptors, their reduced species, and arsenate as well as arsenite that will result from the degradation of an organic carbon source in the sediments. Even though specific biological transformations are allowed to proceed only in zones where they are thermodynamically favorable, the results show that mixing as well as abiotic reactions can make the profiles of individual electron acceptors overlap and/or appear to reverse their expected order.

Key words : Wetland sediments, Geochemistry, Numerical modeling, Arsenic

INTRODUCTION

The fate and transport of many trace metals, metalloids, and radionuclides in porous media are closely linked to the biogeochemical reactions that occur as a result of organic carbon being degraded by different microorganisms using a series of terminal electron acceptors. Throughout the redox profile that develops in such environments, trace metals can be mobilized/immobilized via processes such as reduction/oxidation, sorption/desorption, precipitation/dissolution, and/or the formation of complex ions. Although the work presented here is generic and applies to a wide range of trace metals, metalloids, and radionuclides, for this study, it will focus the simulations specifically on arsenic as a model contaminant.

Arsenic is a ubiquitous contaminant that is, among others, associated with chemical and power industry as well as agriculture. The predominant forms of arsenic in natural water systems are As(V) as H_3AsO_4 (arsenate), and As(III) as H_3AsO_3 (arsenite). Arsenate is dominant in oxic waters, but under reducing conditions is converted to arsenite (Massacheleyn *et al.*, 1991). Like phosphate, arsenate exists mainly in its deprotonated forms at natural pH levels, and is

* Corresponding Author: Tel: 02) 3277-4037, Fax: 02) 3277-3275, E-mail: sookyun@ewha.ac.kr

therefore readily sorbed onto positively charged surfaces of minerals such as Fe (III) oxides (Dzombak and Morel, 1990). Bacteria have been identified which, in environments that are more reduced than nitrate reduction, can use arsenate as a terminal electron acceptor, reducing it to arsenite (Newman *et al.*, 1997a, b; Dowdle *et al.* 1996). Arsenite is the more toxic form of arsenic, and it exists primarily as a neutral dissolved species at ambient pH values, and zones that have a more reducing environment. Compared to arsenate, transport of arsenite is therefore not significantly retarded due to sorption (Gulens *et al.*, 1979), but it has a high affinity to form complexes with sulfides, forming sulfide minerals such as orpiment (As_2S_3).

Given that the transport and bioavailability of many metals and metalloids are affected by complex sets of chemical reactions and physical mechanisms, a general analytical framework has been developed in order to improve our understanding of how the fate and transport of these metals are affected by various biogeochemical and physical transport processes. Because these processes are highly dependent on ambient conditions, the biogeochemical dynamics of arsenic will be different in various environmental settings. Through simulations, this study will focus on two important hydrologic settings, permanen-

tly flooded freshwater sediments, where redox conditions range from highly oxidized to highly reduced, namely wetland sediments without rooted plants and wetland sediments with rooted macrophytes (referred to hereafter as non–vegetated wetland sediments and vegetated wetland sediments, respectively). The objective of this study is to assess the main differences in model development as well as arsenic fate and transport in these various natural conditions.

Common to the modeling approach is that, distinct redox zones will develop as a result of the biodegradation of organic matter and the sequential utilization of different terminal electron acceptors as shown in Table 1. The spatial distribution of these zones will determine where arsenic is reduced/oxidized, sorbed to different solid phases, and/or precipitates. Clearly pH is a key parameter in determining the fate of arsenic and other chemical constituents in the environments, and spatial/temporal pH values will depend on the different biotic and abiotic reactions occurring in each redox zone. Complex microbial and chemical redox reactions could change pH conditions in the aquatic system by producing/consuming acid and base constituents during the decomposition of organic matter. For the purpose of this work, however, pH will be considered a model input and will not be simulated explicitly.

Table 1. Key biogeochemical model stoichiometric relationships.

Layer	Stoichiometric Relationships for the Major Model Redox Reactions*
1.	$(CH_2O)_{106}(NH_3)_{16}(H_3PO_4) + 106\ O_2 \rightarrow 106\ CO_2 + 16\ NH_3 + H_3PO_3 + 106\ H_2O$
a.	$NH_4^+ + 2\ O_2 \rightarrow NO_3^- + H_2O + 2\ H^+$
b.	$2\ Mn^{2+} + O_2 + 2\ H_2O \rightarrow 2\ MnO_2 + 4\ H^+$
c.	$4\ Fe^{2+} + O_2 + 10\ H_2O \rightarrow 4\ Fe(OH)_3 + 8\ H^+$
d.	$H_2S + 2\ O_2 \rightarrow SO4^{2-} + 2\ H^+$
e.	$CH_4 + 2\ O_2 \rightarrow CO_2 + 2\ H_2O$
2.	$(CH_2O)_{106}(NH_3)_{16}(H_3PO_4) + 84.8\ NO_3^- + 84.8\ H^+ \rightarrow 106\ CO_2 + 42.4\ N_2 + 16\ NH_3 + H_3PO_3 + 148.4\ H_2O$
a.	$NO_3^- + 10\ Fe^{2+} + 10\ H^+ \rightarrow NH_4^+ + 10\ Fe^{3+} + 3\ H_2O$
3.	$(CH_2O)_{106}(NH_3)_{16}(H_3PO_4) + 212\ MnO_2 + 424\ H^+ \rightarrow 106\ CO_2 + 212\ Mn^{2+} + 16\ NH_3 + H_3PO_3 + 318\ H_2O$
a.	$MnO_2 + H_2S + 2\ H + \rightarrow Mn^{2+} + S^0 + 2\ H_2O$
b.	$MnO_2 + 2\ Fe^{2+} + 4\ H_2O \rightarrow Mn^{2+} + 2\ Fe(OH)_3 + 2\ H^+$
4.	$(CH_2O)_{106}(NH_3)_{16}(H_3PO_4) + 424\ FeOOH + 848\ H^+ \rightarrow 106\ CO_2 + 424\ Fe^{2+} + 16\ NH_3 + H_3PO_3 + 742\ H_2O$
a.	$2\ Fe(OH)_3 + H_2S + 4\ H + \rightarrow 2\ Fe^{2+} + S^0 + 6\ H_2O$
5.	$(CH_2O)_{106}(NH_3)_{16}(H_3PO_4) + 53\ SO_4^{2-} + 53\ H^+ \rightarrow 106\ CO_2 + 53\ HS^- + 16\ NH_3 + H_3PO_3 + 106\ H_2O$
a.	$SO_4^{2-} + CH_4 + 2\ H^+ \rightarrow H_2S + CO_2 + 2\ H_2O$
6.	$(CH_2O)_{106}(NH_3)_{16}(H_3PO_4) \rightarrow 53\ CO_2 + 53\ CH_4 + 16\ NH_3 + H_3PO_4$

*In these reactions, the organic material is represented by the Redfield stoichiometry, which differs for terrestrial ecosystems (Vitousek *et al.*, 1988), and can be adjusted depending on the characteristics of the sediment organic carbon source, wetland litter, or carbon source injected into the subsurface. To facilitate comparison between the simulations, the same carbon formulation was used in all cases. It should also be noted that sulfur is not included in the Redfield formula and that therefore the sulfur source used here is external from the organic matter.

MODEL FORMULATIONS IN WETLAND SEDIMENTS

A fundamental difference between saturated sediments near the sediment/water interface (non–vegetated and vegetated wetland sediments) and in the subsurface (groundwater environments) is that, at the interface, sedimentation provides a source for new and usually oxidized sediments. This is important, in that the sedimentation process normally provides a source of fresh iron and manganese oxides. Thus, in sedimentary environments, a quasi–steady–state spatial profile can develop containing a reacting solid phase of Mn (IV) and/or Fe (III). In a system where the solid phase is stationary, such as groundwaters, steady–state conditions cannot result in the presence of such reacting solid phases. It should be noted that only a fraction of the Mn (IV) and Fe (III) is bioavailable. Amorphous iron oxide may be bioavailable while crystalline forms are not.

For wetland sediments, an oxidized surface layer of sediment is typically present at the sediment/water interface (Ponnamperuma, 1984; Mitsch and Gosselink, 1993), which is followed by a steep redox gradient, resulting from the different reactions shown in Table 1 proceeding sequentially. Concentration gradients of redox species of more than an order of magnitude over a distance of a centimeter have been observed in different sediments (Brendel and Luther, 1995).

Arsenic may be immobilized due to sorption onto different organic and inorganic soil constituents or due to precipitation. Adsorption of arsenate onto iron and manganese oxides is an important process where the oxidation potential is high. As the system becomes more reduced, iron and manganese oxides are depleted, and trace metals as well as arsenic can desorb and remobilize as a dissolved species, although in the presence of sulfide ions, are usually immobilized as sulfides.

In addition to the processes described above, redox profiles in wetland sediments are also affected by the presence of higher plants. Wetland plants have evolved specialized adaptations to supply oxygen to the roots, and to transfer oxygen from the roots into the surrounding sediment (Armstrong, 1979; Bedford et al., 1991; Mendelssohn, 1993). This transfer of oxygen maintains an oxidizing potential in the rhizosphere, which is important for root survival. It protects roots from phytotoxins, which are common in swamps at low redox potentials, and prevents transport into the root of highly soluble Fe (II) ions by precipitating them at the root surface following oxidation to Fe (III) (Grosse, 1997). The rates of oxygen transfer into wetland sediments can be substantial and highly variable (Armstrong, 1979; Bedford et al., 1991; Brix, 1993; Sorrel, 1994). These rates are dependent on the type of vegetation and root size, as well as the chemical composition and oxygen demand of the sediments (Brix et al., 1996). Oxygen release rates measured for E. sphacelata ranged from non–detection for roots placed in a deoxygenated solution, to $55 \, \mu mol \, h^{-1} \, g^{-1}$ dry weight when placed in a solution with a redox potential of -200 mV (Sorrel et al., 1993). The degree of iron plaque accumulation on roots is highly variable, and depends on the concentration of ferrous iron in solution as well as its complexation with organic ligands and the availability of other exchange sites on different soil mineral and organic fractions (Mendelssohn, 1993). Adsorption of arsenic, as well as other trace metals, can be significantly enhanced in the rhizosphere due to the formation of these iron oxyhydroxide plaques on roots (Otte et al., 1995). In addition to oxygen transfer, evapotranspiration also affects the redox profile of wetland sediments, by inducing advection that changes the vertical flow velocity profile.

SIMULATION OF THE DYNAMICS OF TRACE METALS AND METALLOIDS IN WETLAND SEDIMENTS

Biologically–mediated redox dynamics in fresh– and marine water sediments as well as groundwaters have been simulated in terms of the sequential utilization of different electron acceptors during the biodegradation of sediment organic matter (Rabouille and Gaillard, 1991; Sweerts et al., 1991; Matsunaga et al., 1993; Park and Jaffé, 1996; Wang and Van Cappellen, 1996; Hunter et al., 1998; DiToro, 2001). In many of these studies, it was assumed that the metal is at equilibrium with the surrounding geochemistry. Clearly this is not always the case. Fe (II) for example, can be found in measurable amounts in oxic and nitrate reducing waters, where

it has been transported from zones where Fe (III) is being reduced. Non–equilibrium conditions have therefore been implemented in formulating the cycling of iron and manganese by many of these investigators (e.g., Hunter *et al.*, 1998), and for contaminant trace metals that undergo redox reactions where the metals are kinetically driven towards chemical equilibrium by biological reactions (Smith and Jaffé, 1998) or abiotic reduction (Jardine *et al.*, 1999).

The fundamentals of the model formulation and the generic equations are given in the Appendix. The spatial (vertical in sediments) profiles of fifteen coupled constituents including solid (organic matter, manganese oxides, iron oxides, and orpiment) and dissolved substances (dissolved organic carbon, oxygen, nitrate, sulfate, ammonia, dissolved manganese, dissolved iron, sulfide, methane, arsenate, and arsenite) and their interactions, including phase changes such as precipitation, dissolution, and sorption are described.

To model the profile of the redox conditions in wetland sediments, the model formulations describe the degradation of organic matter and the sequential reduction of electron acceptors, taking into account where appropriate, transport processes such as molecular diffusion, dispersion, bioturbation, irrigation, and advection. Bioturbation and irrigation are described as a mixing process similar to dispersion and molecular diffusion, as discussed by Berner (1980). Bioturbation and irrigation are processes driven by benthic organisms, which are present in wetland sediments. Based on the electron acceptor that is being used by the microorganisms degrading the organic substrate, the spatial domain is divided into six different zones: aerobic respiration, denitrification, manganese reduction, iron reduction, sulfate reduction, and methanogenesis (Park and Jaffé, 1996; 1999). The microbial utilization of the electron acceptors in each of these zones is described by the stoichiometric equations shown in Table 1. For vegetated wetland sediments, effects of plants are included by adding proper source/sink terms to account for organic carbon release (e.g., litter, exudates, root turnover), oxygen release, nutrient uptake (e.g., nitrogen), and evapotranspiration–induced advection. It is assumed here that sedimentation provides a source of fresh bioavailable iron and manganese oxides, as well as particulate organic

carbon at the sediment/water interface.

The microbial degradation of the organic matter is described by a Monod–type formulation. Reactions such as oxygen consumption by reduced compounds (e.g., Mn^{2+}, Fe^{2+}, HS^-) are formulated as second order reactions, and precipitation of Mn^{2+}, Fe^{2+}, with HS^- and other com-

Table 2. Key biotic/abiotic reaction parameters used in the simulation.

Parameters	Values used in simulation*
Maximum specific growth rate when [M yr^{-1}]	
O_2 is the electron acceptor	4.0
NO_3^- is the electron acceptor	1.5
Mn(IV) is the electron acceptor	0.2
Fe(III) is the electron acceptor	0.032
SO_4^{2-} is the electron acceptor	1.8
Half saturation constant of [μM]	
organic carbon	100
O_2	100
NO_3^-	20
Mn (IV)	1
Fe (III)	1
SO_4^{2-}	10
Threshold concentrations [μM] for indicator χ_{eA}	
O_2	0.5
NO_3^-	6
Mn (IV)	1
Fe (III)	5
SO_4^{2-}	15
Biological As reduction rate [yr^{-1}]	130**
Abiotic As oxidation rate [M^{-1} yr^{-1}]	6.0×10^6***
Maximum utilization rate of [yr^{-1}]	
ammonia oxidation (nitrification)	30
Aerobic methane oxidation	10
Half saturation constant of [μM]	
ammonia oxidation (nitrification)	30
Aerobic methane oxidation	10

Second–order rate coefficients for the redox reactions [M^{-1} yr^{-1}]		
Oxidants	Reductants	
MnO_2 (s)	Fe^{2+}	1.0×10^4
MnO_2 (s)	HS^-	8.0×10^5
FeOOH (s)	HS^-	1.0×10^3
O_2 (aq)	XMn^{2+} (ads)	2.1×10^7
O_2 (aq)	XFe^{2+} (ads)	1.6×10^8
O_2 (aq)	Fe^{2+}	2.1×10^7
O_2 (aq)	Mn^{2+}	4.6
O_2 (aq)	HS^-	2.0×10^5
NO_3^-	Fe^{2+}	1.6×10^3
$[SO_4^-]_{total}$	CH_4	1.0×10^4

*Kallin (1999); **Newman *et al.*, 1997b; ***Scott and Morgan, 1995; all other parameters are based on Smith and Jaffé (1998)

pounds such as phosphorus and carbonate (or dissolution of the respective mineral), are formulated as being proportional to the degree of over– or undersaturation as shown in the Appendix. Diffusion and/or advection of different chemical species across redox boundaries, followed by mixing will result in many additional biotic and abiotic redox reactions (e.g., abiotic reduction of MnO_2 by HS^-). The most relevant reactions for the problem at hand and typical rate coefficients have been discussed by several authors (Von Gunten and Zorbist, 1993; Matsunaga *et al.*, 1993; Smith and Jaffe, 1998). Coefficients for the biotic and abiotic reaction rates included in the simulations are given in Table 2. The model formulation allows for an easy incorporation of additional reactions that are identified as being important. Although none of the systems simulated are close to reach chemical equilibrium conditions, the pE at a specific location is approximated to that of the dominant redox couple (Morel and Hering, 1993). The dominant redox couple in each sediment layer is assumed to be given by the half reaction of the respective electron acceptor for organic matter oxidation.

With the computed concentration profiles of the oxidized and reduced electron acceptors, pE, species such as organic carbon and ammonia, and inputted values for the pH and alkalinity, MINTEQA2 (an EPA supported equilibrium chemical speciation model) is applied to determine the chemical speciation under equilibrium conditions for each of a set of specified chemical constituents (e.g., trace metals, metalloids, sulfides) at each location in the sediments. The difference between the actual and these equilibrium concentrations determines how far from equilibrium a reaction is. Although it is not a mechanistically–based formulation, it is convenient to describe the rate at which equilibrium conditions are approached by the product of a rate constant and the gradient given by this concentration difference. This allows a consistent, dynamic formulation for species such as arsenic and all of the other species reacting with it, considering changes in oxidation state, complexation with different ligands, and precipitation. Even though the approach of coupling a transport and chemical speciation model is computationally expensive, it has the advantage of being general and allowing for the easy incorporation/substitution of additional chemical species.

Table 3. Physical and transport parameters used in the simulation.

Parameters	Values used in simulation
domain length [cm]	17.5
infiltration/groundwater velocity [cm yr^{-1}]	50
coefficient of bioturbation [cm^2 yr^{-1}]	150
coefficient of irrigation [cm^2 yr^{-1}]	300
characteristic depth of bioturbation layer [cm]	10.5
characteristic depth of irrigation layer [cm]	10.5
porosity	0.5
dry bulk density of soil [g cm^{-3}]	1.7
pH	6.75
Fe (III) deposition rate [moles cm^{-2} yr^{-1}]	1.0×10^{-3}
Mn (VI) deposition rate [moles cm^{-2} yr^{-1}]	3.3×10^{-4}
carbon deposition rate [moles cm^{-2} yr^{-1}]	5.0×10^{3}
evapotranspiration rate [cm yr^{-1}]	50
depth of rhizosphere [cm]	8.5

Sorption of arsenate, as well as the other species simulated, onto solid organic carbon is described by a linear sorption isotherm, and sorption onto manganese and iron oxide by the double layer surface complexation model, accounting for interactions among these species (Dzombak and Morel, 1990).

RESULTS

A series of simulations were conducted to compare the dynamics of arsenic in non–vegetated and vegetated wetland sediments. Physical and transport parameters used in these simulations are given in Table 3. For the sedimentary environments, constant concentration boundary conditions were set for the dissolved constituents at the water/sediment interface, and constant flux conditions for the solid components. Zero gradient conditions were set for the bottom of the domain. Zero gradient boundary conditions do affect the simulated profiles near the bottom of the domain, and changes in the gradient of some profiles near the bottom of the domain can be attributed to these boundary conditions. In wetland sediments, one might have either groundwater recharge or discharge. The results shown here will focus on surface water entering the sediments only.

The effect of roots on the dynamics of electron acceptors and arsenic in sediments is compared at first. Figure 1 and 2 show the respective non–
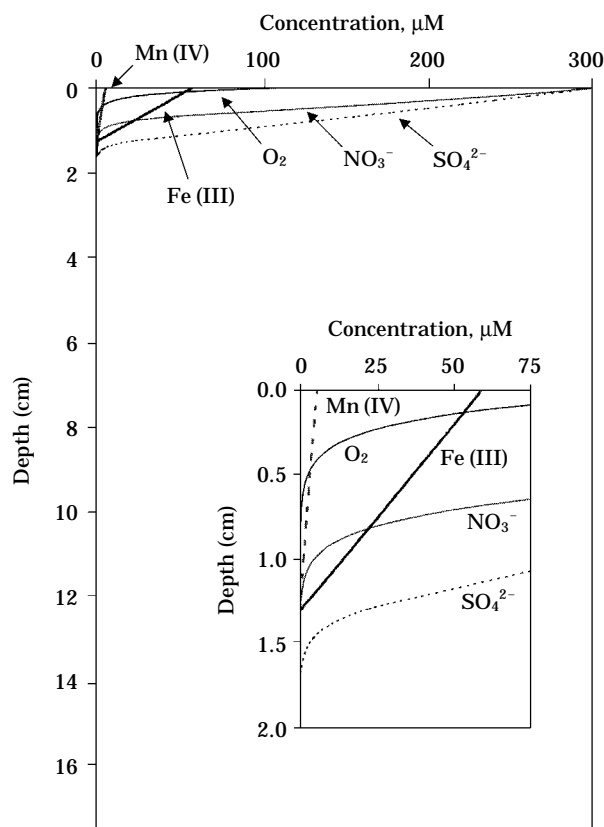
Concentration, μM

Fig. 1. Simulated concentration profiles of terminal elec-
tron acceptors in non–vegetated wetland sedi-
ments.

Fig. 2. Simulated concentration profiles of terminal elec-
tron acceptors in vegetated wetland sediments.

vegetated and vegetated wetland sediment pro-
files of electron acceptors being consumed during
the degradation of organic matter, while Figures
3 and 4 show the profiles of their corresponding
reduced form as well as ammonia in non–vege-
tated and vegetated wetland sediments, respec-
tively (methane concentration is not shown).
Simulations were conducted for a series of oxy-
gen–release and evapotranspiration rates. For
the simulations shown here, when roots are pre-
sent, oxygen is being released into the sediments
at a rate of 3 g O_2 m^{-2} day^{-1}, and evapotrans-
piration is 50 cm yr^{-1}. Root density was assumed
to decrease as a cosine function from the water/
sediment interface to a depth of 8 cm. Oxygen
release, as well as water uptake as a function of
depth was assumed to be proportional to the root
density.

As can be seen by comparing Figures 1 and 2,
the average oxygen concentration in the rhizo-
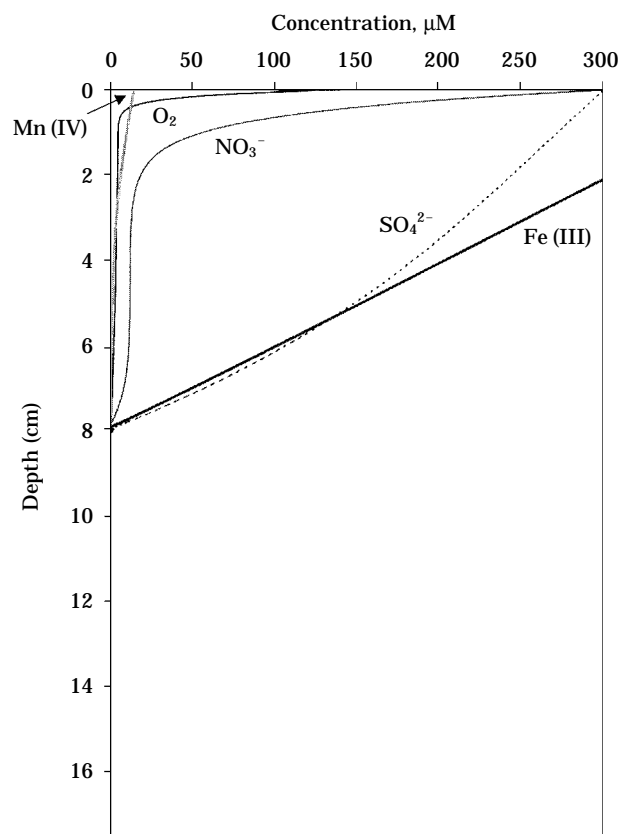sphere (upper 8.5 cm) of vegetated wetland sedi-

ments is higher than that in non–vegetated wet-
land sediments (no roots present). The increased
oxygen concentration can cause that the oxidized
species (NO$_3^-$, Mn (IV), Fe (III), and SO$_4^{2-}$) to be
transported deeper into the wetland sediments
before being used as an electron acceptor. Com-
pared to sediments where no roots are present,
for the wetland case (with roots), this results in a
decrease in the concentration gradient of dissolv-
ed oxygen at the water/sediment interface and
increased depth of depletion. Conversely, the
reduced species shown (Mn^{2+}, Fe^{2+}, and HS$^-$) are
being produced deeper in the vegetated wetland
sediments, resulting in a decreased gradient at
the water/sediment interface, and hence a reduc-
ed flux of these species into the water column
(see Figs. 3 and 4). It is interesting to note the
very sharp Fe^{2+} peak in these profiles. Actual Fe
(III) reduction occurs only at the specific depths
associated with these Fe^{2+} peaks, and the rapid
disappearance of the dissolved Fe^{2+} below the Fe
(III) reduction zone is due to the precipitation of

Fig. 3. Simulated concentration profiles of reduced species in non–vegetated wetland sediments.
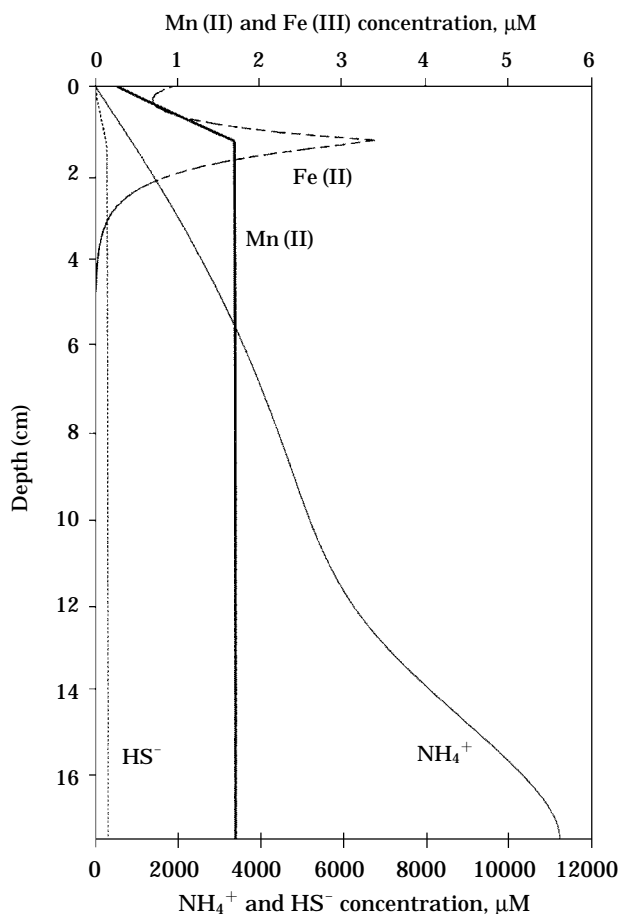
Fig. 4. Simulated concentration profiles of reduced species in vegetated wetland sediments.

FeS. These Fe^{2+} profiles are extremely sensitive to the precipitation rate, and measurements of these rates under different environmental conditions are needed. For the simulations shown in this work, a precipitation rate (k_s, as defined in the appendix) of $40\,M^{-1}\,yr^{-1}$ was selected (M is the molarity.).

Because evapotranspiration induces flow in the sediments towards the roots, the effect of evapotranspiration on these profiles is even more marked. Evaporation–induced advection increases the flux of dissolved species (O_2, NO_3^-, SO_4^{2-}) from the water/sediment interface into the sediment. This increases the overall mass of available electron acceptors entering the sediments to the microorganisms degrading the organic matter. Furthermore, since a given mass of water is withdrawn from the rhizosphere due to evapotranspiration, a mass balance for the individual spec-
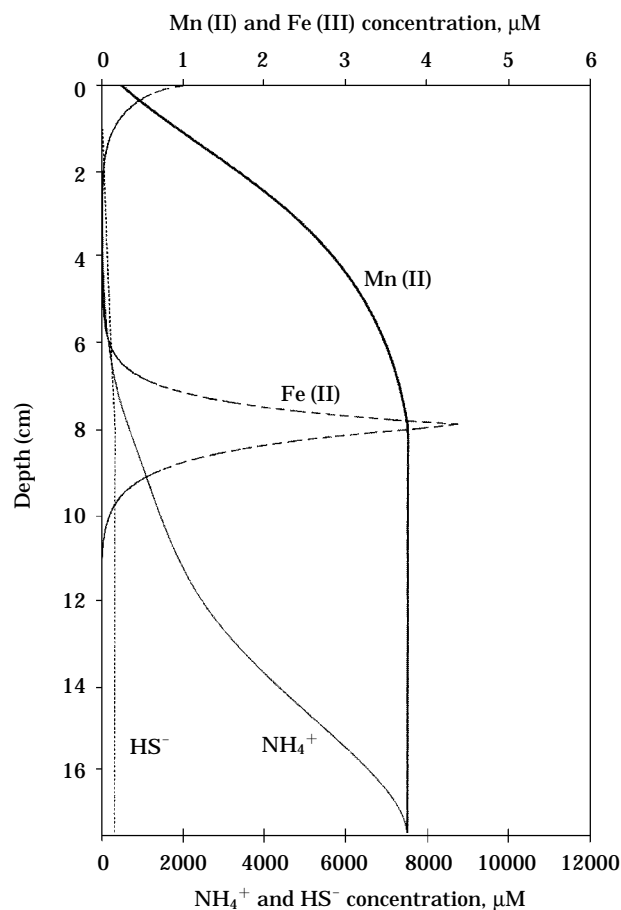
ies dictates that their concentration increases due to this water withdrawal. This effect can be seen clearly for the reduced Mn, Fe and S, which all increase in concentration throughout the whole rhizosphere, reaching concentrations that are significantly higher than for the case with no roots present (compare Figs. 3 and 4).

Nitrate and ammonia uptake by plants was described by a Fickian expression, proportional to the concentration difference between the ambient concentration and a specified cutoff concentration. The nitrate and ammonia uptake rate coefficients were chosen to result in an annual biomass growth of $3,000\,g/m^2$ assuming 2.5% nitrogen by weight. Additionally, sorption of NH_4^+ to the sediments was assumed to follow a linear sorption isotherm. Therefore, evapotranspiration affects the nitrate profile only in terms of increasing the overall flux into the sediments.
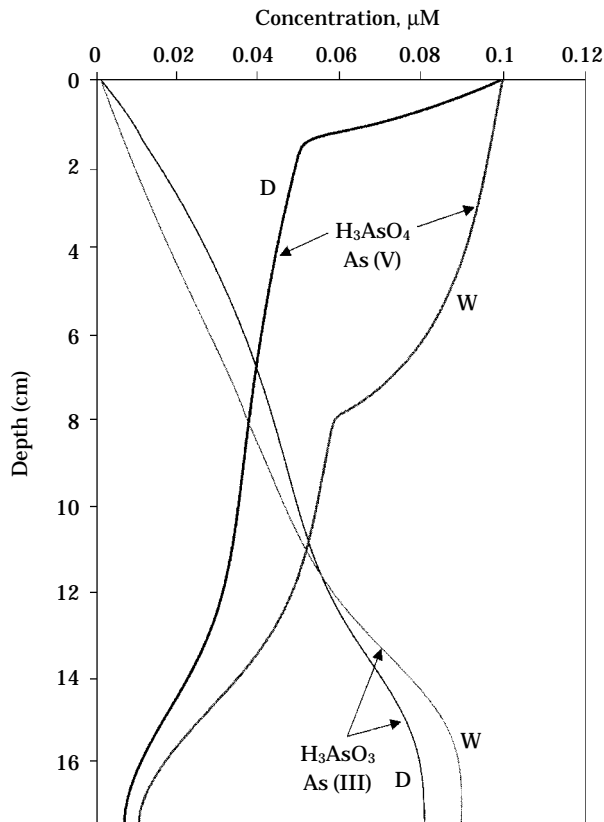
Fig. 5. Simulated concentration profiles of arsenate (As (V)) and arsenite (As (III)) in non-vegetated wetland (D) and vegetated wetland (W) sediments.

Higher oxygen releases into the sediments by roots results in a larger conversion of ammonia into nitrate. The combined effect of increased nitrification and uptake by plants results in a significant decrease in the ammonia concentration in the rhizosphere of vegetated wetland sediments as compared to the non-vegetated wetland sediment case.

Figure 5 shows the simulated profiles of dissolved arsenate and dissolved arsenite for non-vegetated and vegetated wetland sediments. These profiles show that in non-vegetated wetland sediments much steeper gradients for arsenate and arsenite can develop at the sediment/water interface, when macrofaunal irrigation effects are not intense, as compared to the vegetated wetlands case where due to the effects of plant roots the profiles are less steep. Therefore, a key impact of the root activity is to decrease the flux of dissolved arsenate entering the sediments from the overlaying water column as well

as the flux of the more toxic arsenite that is returned into the water column from the sediments. These fluxes are altered in their magnitude not only because of the change in the concentration gradients, but also due to the increase in the advective flow induced by evapotranspiration. Since these are steady state simulations, the dissolved–phase fluxes are not affected by the increased sorption of arsenate onto the larger amounts of iron and manganese oxides in wetland sediments. However, when the total flux of arsenic, including the sorbed phase, is considered, the presence of plants tends to increase the amount of arsenic buried in the sediments. If temporal spikes in the water column's arsenic concentration were considered, sorption would play a larger role in decreasing the dissolved–phase concentration and the effect of roots on buffering the flux of arsenite into the water column would be even larger. It should be noted that a wide range of root density distribution can be expected depending upon the type of wetland vegetation, and that different root density distributions will affect the individual concentration profiles.

As discussed earlier, arsenate can act as an electron acceptor for certain bacteria during the degradation of organic matter, and the same generic formulation was used for arsenate reduction as for the other dissolved electron acceptors. As opposed to the major electron acceptors described in the model, arsenate reduction was allowed to proceed in parallel with the reduction of the other electron acceptors after nitrate has been consumed. For this reason arsenate reduction proceeds even when the environment becomes highly reduced and methanogenesis occurs, such as deep in the sediments where sulfate has been consumed. Further research is necessary to establish if there is a lower redox limit for the reduction of arsenate. The effect of the current formulation on arsenic reduction can be seen in Figure 5, where arsenate concentration steadily decreases and arsenite concentration increases with depth or time. Even though microbiological arsenate reduction is not initiated until all the nitrate has been consumed, Figure 5 shows that a concentration gradient for arsenate and arsenite extends from the water/sediment interface through the aerobic and nitrate reducing zones. This gradient develops due to mixing (mainly bioturbation and irrigation) and does not imply

that arsenate is being reduced in these zones.

DISCUSSION

The results presented here illustrate a methodology capable of simulating the biogeochemical dynamics of trace metals and metalloids, specifically arsenic, in wetland sediments. Redox profiles, which develop in sediments in response to the utilization of different terminal electron acceptors during the biodegradation of organic carbon, were simulated, and coupled with the dynamics of arsenic as it is transported across the different redox zones. The key physical processes that have been considered here are sedimentation, enhanced oxygen transport by roots, transport–induced advection, and differences in mixing. The simulation results have shown that these processes have significant effects on the concentration profiles of all the chemical species simulated and how these profiles may overlap with each other. For a non–stationary solid matrix, as is the case for sediments where the sediment/water interface is moving over time due to sedimentation, a steady–state formulation will yield zones where manganese and iron reduction are occurring. A steady–state formulation may therefore be appropriate to simulate a long–term quasi–steady–state in sedimentary environments. Given that sorption of arsenate to sorbents such as iron oxides affects the fate of arsenic in the environments, it is extremely important to properly simulate the dynamics of these sorbents. Significant amounts of manganese and iron oxides can build up in the rhizosphere of wetland sediments, which can have an important effect on the overall immobilization of arsenic in wetlands.

A common feature used in the formulations examined here is that individual chemical species are not assumed to be at chemical equilibrium. Chemical equilibrium calculations are only used to determine the deviation from equilibrium conditions, based on which a kinetic formulation is implemented. This formulation allows different species to coexist. For example, as shown in all of presented simulations, species such as Fe^{2+} do coexist with other more oxidized species such as NO_3^-. This is commonly observed in sediments, and could not be simulated if equilibrium formulations were implemented.

These reaction kinetics can have significant impacts on the individual chemical profiles. As can be seen from the insert in Figure 1, when the water flow is from the oxidized zone to the reduced zone, the electron acceptors are depleted sequentially in the order shown in Table 1. Conversely, when the water flows from reduced to more oxidized zones (e.g., groundwater for larger distances from the origin or groundwater discharge type wetlands), the various biotic and abiotic reactions occurring simultaneously can alter the spatial sequence of the profiles of the electron acceptors from that described in Table 1. This, as well as the overlapping concentration profiles near the water/sediment interface, illustrates that knowledge of the electron acceptor profiles alone does not provide adequate information to identify the zones where a specific microbiological process is occurring. Additional measurements such as the partial pressure of H_2, which can define the bacteria capable of existing at that partial pressure (e.g., Lovley and Goodwin, 1998), might be required to better assess what degradation process is occurring at a given location. Such measurements may also help to more efficiently compare the accuracy of the model simulations to field data.

The simulated concentration profiles of electron acceptors in non–vegetated wetland sediments shown here compare well to a series of profiles measured in lake sediments and described in Smith and Jaffé (1998). This was achieved using rate coefficients consistent with those reported in the literature (Smith and Jaffé, 1998; Kallin, 1999). Yet accurate model verification, especially for field conditions, is difficult to achieve due to the complexity of these models and the large number of model coefficients.

Given the limitations in model validation, the utility of biogeochemical models such as those presented here is mainly as a scientific tool to understand variable interactions, and to be used as an aid in interpreting trends in field observations. For example, by comparing the simulations for non–vegetated sediments to those for vegetated sediments, one can gain a reasonable understanding on how the colonization of aquatic plants will affect the fluxes or distributions of trace metals or metalloids in a shallow lake.

Finally, it should be noted that the one–dimensional models presented here do not allow for heterogeneities in the porous media where loca-

lized differences in the microbiological processes can develop. This is expected to occur in natural settings and would contribute even more to the smearing of specific concentration profiles.

Appendix – Formulations of Model Equations
  Mass balance equations for dissolved species

$$\frac{\partial}{\partial t}\,(\phi\,[1+K_i^{eff}])\,C_i^{aq} = -\frac{\partial}{\partial z}\,[(V(z)-W)\,\phi\,C_i^{aq}]$$
$$+W\frac{\partial\,(K_i^{eff}\,\phi\,C_i^{aq})}{\partial z}+\frac{\partial}{\partial z}\Big[(D_{hi}+D_b(z)$$
$$+D_{irr}(z))\cdot\frac{\partial\phi C_i^{aq}}{\partial z}+D_b(z)\,\frac{\partial\,(K_i^{eff}\phi C_i^{aq})}{\partial z}\Big]+\sum R_i$$

ϕ : porosity
K_i^{eff} : effective partition coefficient for the equilibrium adsorption of species i [M/M]
C_i^{aq} : concentration of the dissolved species i [M/V]
V : infiltration velocity of water (positive down) in sediments [L/T]
z : distance from the sediment/water interface [L]
W : velocity of the sediment/water interface (from deposition: negative values corresponding to accumulation of sediment) [L/T]
D_{hi} : coefficient of hydrodynamic dispersion (mechanical dispersion+molecular diffusion) of species i [L²/T]
D_b : coefficient of bioturbation (mixing of sediment by aquatic and benthic organisms) [L²/T]
D_{irr} : coefficient of irrigation (mixing of porewater by aquatic and benthic organisms) [L²/T]
$\sum R_i$: sum of consumption/production of species i by biotic/abiotic reactions [M/VT]

  The effective partition coefficient for species i, K_i^{eff}, is defined as

$$K_i^{eff}=\frac{(1-\phi)\cdot[\text{total adsorbed concentration of component species i}]}{\phi\cdot[\text{total dissolved concentration of component species i}]}$$

  Mass balance equations for solid species

$$\frac{\partial}{\partial t}\,[(1-\phi)\,C_i^s]=W\frac{\partial}{\partial z}\,[(1-\phi)C_i^s]$$
$$+\frac{\partial}{\partial z}\Big[(1-\phi)D_b(z)\cdot\frac{\partial C_i^s}{\partial z}\Big]+\sum R_i$$

C_i^s : concentration of the solid species i [M/V]

  The bioturbation and irrigation coefficients were assumed to decrease with depth according to:

$$D_b=\frac{D_b^{\,0}}{[1+\exp\{z-z_b\}]},\quad D_{irr}=\frac{D_{irr}^{\,0}}{[1+\exp\{z-z_{irr}\}]}$$

$D_b^{\,0}$, $D_{irr}^{\,0}$: coefficients of bioturbation and irrigation at the sediment/water interface in sediments [L²/T]
z_b, z_{irr} : characteristic depths for bioturbation and irrigation [L]

  The rate of oxidation of organic carbon, C_c, by a given terminal electron acceptor of concentration C_{eA}:

$$R_C^{eA}=-\chi_{eA}\mu_{meA}\Big(\frac{C_{eA}}{K_{seA}+C_{eA}}\Big)\Big(\frac{C_C}{K_{seA,C}+C_C}\Big)$$

χ_{eA} : indicator coefficient (1 when this electron acceptor is being utilized, and 0 when it is not)
μ_{meA} : maximum rate of carbon oxidation via this electron acceptor [M/VT]
K_{seA} : half-saturation coefficient for the electron acceptor [M/V]
$K_{seA,C}$: half-saturation coefficient for the carbon substrate (for consumption of this electron acceptor) [M/V]

  The rate of consumption of a given terminal electron acceptor, which equals the rate of production of its corresponding reduced species:

$$R_{eA}=-\alpha_{eA}\cdot R_C^{eA}$$
$$=-\alpha_{eA}\chi_{eA}\mu_{meA}\Big(\frac{C_{eA}}{K_{seA}+C_{eA}}\Big)\Big(\frac{C_C}{K_{seA,C}+C_C}\Big)$$
$$=-R_{\text{corresponding reduced species}}$$

α_{eA} : stoichiometric coefficient representing the ratio of the number of moles of a given electron acceptor required to oxidize one mole of organic carbon

  The rate of oxidation of ammonia and corresponding production of nitrate and consumption of oxygen:

$$R_{NH_3}^{O_2}=-\alpha_{NH_3,O}\mu_{meA,O_2}\cdot\Big(\frac{C_{NH_3}}{K_{s,NH_3}+C_{NH_3}}\Big)\Big(\frac{C_{O_2}}{K_{s,O_2}^{NH_3}+C_{O_2}}\Big)$$

  Second-order rate of redox reactions:
* Rates of oxidation of dissolved reduced species i (e.g., Mn^{2+}, Fe^{2+}, HS^-, CH_4) by oxidant j:

$$R_i^j=\mu_{j,i}C_jC_i$$

$\mu_{j,i}$: stoichiometric coefficient representing the

ratio of the number of moles of a given electron acceptor required to oxidize one mole of organic carbon

* Rates of oxidation of adsorbed Fe (II) and Mn (II) (represented as a function of the concentration of the reduced metal adsorbed onto Mn (IV) oxides):

$$R_{M^{2+}}^{ox} = \mu_{M^{2+}}^{ox}[XO_2 \cdot M^{2+}] \cdot C_{O_2}$$

$\mu_{M^{2+}}^{ox}$: rate coefficient for oxidation of adsorbed metal

$[XO_2 \cdot M^{2+}]$: concentration of metal M^{2+} adsorbed onto metal oxides, XO_2 (the adsorption is calculated by the equilibrium speciation model)

For a given solid, S, composed of N_s species, the net rate of precipitation, R_s^{net}

$$R_s^{net} = k_s \cdot \left(\prod_i^{N_s} [FIA_i]^{\alpha_{i,s}} - K_{sp}^S \right)$$

k_s : precipitation rate coefficient specified for solid S [reaction dependent, for $N_s = 2$, M^{-1} yr^{-1}]

FIA_i : dissolved free ion activity of component i [M/VT]

$\alpha_{i,s}$: stoichiometric coefficient of the i-th component of solid S

K_{sp}^S : equilibrium solubility product for solid S [reaction dependent, for $N_s = 2$, M^2/V^2]

Integration of the role of plants in wetland sediment model

* Variable velocity field (described as the superposition of a groundwater infiltration velocity field and an evapotranspiration-induced velocity field)

$$V(z) = V_{Inf} + \alpha ET \cdot w(z)$$

V_{Inf} : groundwater infiltration velocity [L/T]
α : proportionality constant (typically assumed as 0.5)
ET : total annual evapotranspiration [L/T]
w(z) : a normalized root density function

$$\left(= \cos\left[\frac{\pi}{2} \cdot \frac{z}{z_{rhiz}} \right] \right)$$

z_{rhiz} : depth of the rhizosphere [L]

* Oxygen diffusion in the rhizosphere:

$$Oxysource\ (z) = \delta \cdot \frac{a}{z_{rhiz}} \cdot Rhizload \cdot w(z)$$

δ : an indicator function (1 when $z < z_{rhiz}$, 0 otherwise)
a : normalization factor
Rhizload : the oxygen loading [M/L^2T]

* Nitrogen uptake:

$$Nitup\ (z) = \delta \cdot ET \cdot w(z) NitMT_0 (C_0^{NO_3} - C^{NO_3}(z))$$

Nitup (z) : nitrate uptake rate [M/VT]
$NitMT_0$: baseline mass transfer rate coefficient [1/T]
$C_0^{NO_3}$: specified minimum nitrate concentration below which uptake stops [M/V]
$C^{NO_3}(z)$: aqueous nitrate concentration [M/V]

REFERENCES

Armstrong, W. 1979. Aeration in higher plants. *Adv. Bot. Res.* **7**:226-332.
Bedford B., D.R. Bouldin and B.D. Beliveau. 1991. Net oxygen and carbon dioxide balances in solutions bathing roots of wetland plants. *J. Ecol.* **79**: 943-959.
Berner, R.A. 1980. Early Diagenesis; A Theoretical Approach. Princeton University Press, Princeton, NJ, 241 p.
Brendel, P.J. and G.W. Luther, III. 1995. Development of a gold amalgam voltametric microelectrode for the determination of dissolved Fe, Mn, O₂, and S (-II) in porewaters of marine and freshwater sediments. *Environ. Sci. Technol.* **29**:751-761.
Brix, H. 1993. Macrophyte-mediated oxygen transfer in wetlands: Transport mechanisms and rates, p 391-398. *In*: Constructed wetlands for water quality improvement (G.A. Moshiri, eds.). Lewis Publishers, Inc., Boca Raton, FL.
Brix, H., B.K. Sorrel and H.H. Schierup. 1996. Gas fluxes by in situ convective flow in Phragmites australis. *Aquatic Botany* **54**:151-163.
DiToro, D.M. 2001. Sediment Flux Modeling, John Wiley & Sons, Inc., New York, NY.
Dowdle, P.R., A.M. Laverman and R.S. Oremland. 1996. Bacterial dissimilatory reduction of arsenic (V) to arsenic (III) in anoxic sediments. *Appl. Environ. Microbiol.* **62**:1164-1669.
Dzombak, D.A. and F.M.M. Morel. 1990. *Surface Complexation Modeling: Hydrous Ferric Oxide*. John Wiley, New York, NY.
Gulens, J., D.R. Champ and K.E. Johnson. 1979. Influence of redox environments on the mobility of arsenic in ground water, p. 81-95. *In*: Chemical Modeling in Aqueous Systems (E.A. Jenne, eds.). Am. Chem. Soc., Symp. Ser. 93.
Grosse, W. 1997. Gas transport in trees. *In*: Con-

tributions to Modern Tree Physiology, p. 57–74. (H. Renneberg, W. Eschrich, and H. Ziegler, eds.). Backhuys Publishers, Leiden, Netherlands.

Hunter, K.S., Y. Wang and P. Van Cappellen. 1998. Kinetic modeling of microbially–driven redox chemistry of subsurface environments: coupling transport, microbial metabolism and geochemistry. *J. Hydrol.* **209**: 53–80.

Jardine, P.M., S.E. Fendorf, M.A. Mayes, L.L. Larsen, S.C. Brooks and W.B. Bailey. 1999. Fate and transport of hexavalent chromium in unsaturated heterogeneous soil. *Env. Sci. Technol.* **33**: 2939–2944.

Kallin, P.L. 1999. Modeling the fate and transport of trace metal contaminants in natural and constructed surface flow wetlands. Ph.D. Dissertation, Princeton University.

Lovley, D.R. and S. Goodwin. 1988. Hydrogen concentration as an indicator of the presence of the predominant terminal electron–accepting reaction in aquatic sediments, *Geochim. Cosmochim Acta*, **52**:2993–3003.

Massacheleyn P.H., R.D. Delaune and W.H. Patrick. 1991. Effect of redox potential and pH on arsenic speciation and solubility in contaminated soil. *Environ. Sci. Technol.* **25**:1414–1419.

Matsunaga, T., G. Karametaxas, H.R. Von Gunten and P.C. Lichtner. 1993. Redox chemistry of iron and manganese minerals in river recharged aquifers: A model interpretation of a column experiment. *Geochim. Cosmochim Acta*, **57**:1691–1704.

Mendelssohn, I.A. 1993. *Factors controlling the formation of oxidizing root channels: a review and annotated bibliography. Tech. Report WRP–DE–5.* US Army Engineer Waterways Experiment Station.

Mitsch, W.J. and J.G. Gosselink. 1993. *Wetlands*, 2nd ed. Van Nostrand Reinhold Co., New York, NY.

Morel, F.M.M. and J.G. Hering. 1993. *Principles and Applications of Aquatic Chemistry*. J. Wiley & Sons, New York, NY.

Newman, D.K., T.J. Beveridge and F.M.M. Morel. 1997a. Precipitation of Arsenic Trisulfide by Desulfotomaculum auripigmentum, *Appl. Env. Microbiol.*, **63**:2022–2028.

Newman, D.K., E.K. Kennedy, J.D. Coates, D. Ahmann, D.J. Ellis, D.R. Lovley and F.M.M. Morel. 1997b. Dissimilatory arsenate and sulfate reduction in Desulfotomaculum auripigmentum sp. nov. *Arch. Microbiol.* **168**:380–388.

Otte, M.L., C.C. Kearns and M.O. Doyle. 1995. Accumulation of arsenic and zinc in the rhizosphere of wetland plants. *Bull. Environ. Contam. Toxicol.* **55**:154–161.

Park, S.S. and P.R. Jaffé. 1996. Development of a redox potential model for the assessment of post-depositional heavy metal mobility, *Ecological Modelling* **91**:169–181.

Park, S.S. and P.R. Jaffé. 1999. A numerical model to estimate sediment oxygen levels and demand, *J. Environ. Qual.* **28**:1219–1226.

Ponnamperuma, F.N. 1984. Effects of flooding on soils, p. 10–46. *In*: Flooding and Plant Growth (T. T. Kozlowki, eds.), Academic Press, New York, NY.

Rabouille, C. and J.-F. Gaillard. 1991. A coupled model representing the deep–sea organic carbon mineralization and oxygen consumption in surficial sediments, *J. Geophys. Res.* **96**:2761–2776.

Scott, M.J. and J.J. Morgan. 1995. Reactions on oxide surfaces, 1, Oxidation of As (III) by synthetic birnessite. *Environ. Sci. Technol.* **29**:1898–1905.

Smith, S.L. and P.R. Jaffé. 1998. Modeling the transport and reaction of trace metals in water–saturated soils and sediments. *Water Resour. Res.* **34**: 3135–3147.

Sorrel, B.K., H. Brix and P.T. Orr. 1993. Oxygen exchange by entire root systems of *Cyperus involucratus and Eleocharis sphacelata. J. Aquatic Plant Management* **31**: 24–28.

Sorrel, B.K. 1994. Airspace structure and mathematical modelling of oxygen diffusion, aeration and anoxia in *Eleocharis sphacelata* R. Br. roots. *Aust. J. mar. Freshwater Res.* **45**:1529–1541.

Sweerts, J.R.A., M–J. Bar–Gillissen, A.A. Cornelese and T.E. Cappenberg. 1991. Oxygen–consuming processes at the profundal and littoral sediment–water interface of a small meso–eutrophic lake (Lake Vechten, the Netherands), *Limnol. Oceananography* **36**:1124–1133.

Vitousek, P.M., T. Fahey, D.W. Johnson and M.J. Swift. 1988. Element interactions in forest ecosystems–succession, allometry and input–output budgets. *Biogeochemistry* **5**:7–34.

Von Gunten, U. and J. Zobrist. 1993. Biogeochemical changes in groundwater infiltration systems: Column studies. *Geochim. Cosmochim. Acta* **57**:3895–3906.

Wang, Y. and P. Van Cappellen. 1996. A multicomponent reactive transport model of early diagenesis: Application to redox cycling in coastal marine sediments, *Geochim. Cosmochim. Acta* **60**: 2993–3014.

<국문적요>

습지 퇴적물에서 비소의 성상과 이동 모의에 관한 수학적 모형

왕 수 균* · 박 석 순

(이화여자대학교 환경학과)

습지에서 중금속이나 방사성 물질의 성상과 이동은 전자수용체와 유기탄소를 이용하는 미생물의 대사작용의 결과로 나타나는 지질화학적 작용과 밀접한 관계를 가지고 있으며, 이러한 지질화학적 반응의 공간적인 분포는 주변 환경의 특성에 의해 영향을 받게 된다. 습지에서의 이러한 현상을 수학적으로 모의하기 위하여 식물의 존재 여부에 따른 퇴적물 내에서의 중금속 거동에 대한 일반적인 수학적 모형을 개발하였다. 본 모형에서 고려되는 주요 기작은 습지에서의 침적과 식물 뿌리의 존재가 퇴적물 내 지질화학적 반응과 이송 기작 및 혼합과정에 미치는 영향 등이며, 정상상태에 관한 수식들이 퇴적물 환경의 모의에 적용되었다. 수치모의 실험의 결과에 따르면, 열거된 물리학적 기작들이 미생물의 유기 탄소원 분해작용의 결과로 나타나는 일련의 전자수용체, 그에 따른 반응물, 모형에서 고려된 중금속 물질인 비소 등 퇴적물내 화학 물질들의 수직적 분포에 중요한 영향을 미치는 것으로 나타났다. 또한 본 모형에서는 특정한 생물학적 변환 과정이 열역학적으로 호의적인 영역에서만 발생하는 것으로 고려되었음에도, 비생물학적 작용과 혼합 기작에 의하여 각각의 전자수용체 분포의 수직적 중첩이나 역전 등 현장에서 실제 관측되는 현상 들을 잘 모사할 수 있었다.